- 1 Synthesis and Catalytic Testing of Lewis Acidic Nano-MFI Zeolites for the Epoxide Ring
- 2 **Opening Reaction with Alcohol**
- 3 **Authors:** Aamena Parulkar, Rutuja Joshi, Nitish Deshpande, Nicholas Brunelli\*
- 4 Address: William G. Lowrie Department of Chemical and Biomolecular Engineering, 151 W.
- 5 Woodruff Ave, Columbus, OH USA 43210
- 6 Authors contributed equally

7 \*Corresponding author: <u>brunelli.2@osu.edu</u>; Twitter: @OSUChemEProfBru

# Abstract

Zeolites have well-defined pores that can impart shape selectivity, but can also cause
diffusion limitations, reducing catalytic performance. While several strategies have been
investigated to overcome diffusion limitations for Brønsted acidic zeolites, limited research has
investigated modifying material properties for Lewis acidic zeolites. In this work, diffusion
limitations for catalytic reactions are overcome through the low temperature synthesis of
nanozeolites containing Lewis acidic tin sites. The growth of the tin-substituted zeolites is
monitored using dynamic light scattering, showing that including tin as a heteroatom at a 200:1
(Si:Sn) in the zeolite synthesis gel does not impact the zeolite growth rate. While similar growth
rates are observed for pure silica and tin-substituted MFI, the low temperature synthesis methods
result in low tin incorporation that can be overcome through adding more tin precursor to the
synthesis gel while still producing nanoparticles. The nano-sized zeolites are demonstrated to
overcome apparent diffusion limitations that conventional Sn-substituted zeolite MFI encounter
for the epoxide ring opening reaction with alcohol. Indeed, conventional Sn-MFI materials can
catalyze the ring opening of 1,2-epoxyhexane with methanol and achieve only 55% conversion
after 24 hours; the nano Sn-MFI zeolites achieve >95% conversion in the same amount of time.
Catalyst reuse experiments demonstrate that the nano zeolite does not leach Sn, but that organic
accumulation in the pores causes loss in apparent catalytic activity. The organic can be removed
through calcination, enabling recovery of the catalytic activity. Overall, engineering of zeolites
with reduced crystal size provides an efficient route to overcome diffusion limitations of bulky
molecules.

Keywords: Epoxide Ring Opening with Alcohol; Lewis Acid Zeolite; Sn-MFI; Nano Zeolite

#### 1. Introduction

Catalytic material design plays an important role in creating highly active [1–3] materials as well as in making more efficient and sustainable processes. Important materials innovations continue to emerge such as Lewis acid substituted zeolites that led to new directions for these important heterogeneous catalytic materials [4–9]. These materials are capable of an impressive array of chemical transformations, including Baeyer Villiger oxidation,[10] Meerwin–Ponndorf–Verley (MPV) reaction [11], olefin epoxidation [12], aldol condensation [13], and sugar isomerization [14] and epimerization reactions [15] for biomass conversion. The expanding scope of catalytic transformations can be limited because of material properties such as pore size [16]. Indeed, the narrow pores of zeolites can be advantageous for shape selective catalysis, but can also be limiting if the pores cause diffusion limitations [17]. Bulky substrates and products tend to diffuse slowly in zeolite pores, resulting in an apparent reaction rate that is much slower than the intrinsic reaction rate or even result in catalyst deactivation through pore blockage. To enable the broadest scope of chemical transformations, it is important to develop material design and synthesis strategies that can produce Lewis acidic catalysts to overcome limitations such as diffusion.

Synthetic methods have been developed to overcome diffusion limitations through reducing the path length for diffusion inside the micropores. Two common approaches to reduce the diffusion path length involve synthesis of hierarchical zeolites and synthesis of nano zeolites. Hierarchical zeolites are materials that in addition to microporosity have mesoporosity that effectively reduces the diffusion length to the catalytic site. Hierarchical zeolites can be synthesized using bottom up and top down approaches that involve templating and non-templating methods, respectively [18]. Templating methods use surfactants or carbon templates such as carbon black in the synthesis to generate mesopores in the final product [19–21]. Non-

templating methods such as desilication [22] or delamination [23] selectively dissolve the zeolite framework through extraction of constituent species from the framework of zeolite resulting in interconnected voids in the material [24,25]. The simplicity of the synthetic methods is attractive and merits consideration, provided that challenges with structural integrity resulting from the creation of mesopores can be addressed [26,27].

An alternative strategy to reduce the effective diffusion path length is to reduce the size of particles to produce nano zeolites [28]. Nano zeolites can be synthesized in two different morphologies such as nanosheets and nano crystals. Ryoo and co-workers demonstrated that appropriately designed bifunctional structure directing agents (SDAs) can direct the formation of ultrathin zeolite sheets with a thickness of 2 nm [29]. In addition to exhibiting excellent thermal stability and long lifetime [29], these materials can be modified with Lewis acidic species to achieve higher catalytic activity than conventional Sn-MFI zeolites [30]. However, the synthesis requires a special SDA, increasing the complexity of the material synthesis. Synthesis of zeolite nanocrystals using commercial SDA would be beneficial to expand the reaction scope of zeolites.

While a non-commercial SDA is required for nanosheet synthesis, zeolite nanocrystals can be obtained through modifying synthesis parameters, including silica source, pressure, time, heating method (microwave or sonication), and synthesis temperature [27,31–38]. One interesting approach that produced pure silica zeolites with the MFI structure involved using lower temperatures to reduce overall particle growth [34,35]. Monitoring particle growth with dynamic light scattering (DLS), it was observed for pure silica materials that crystalline, microporous particles of size 57 or 96 nm can be formed at synthesis temperatures of 60°C and 100°C, respectively.

This previous work focused on forming pure silica materials that are not catalytic, and other recent work has examined aluminosilicates that have Brønsted acidity [39]. For many

emerging applications, it is desirable to have materials with Lewis acidic sites, but creating nano zeolites with Lewis acidic sites could be potentially challenging since heteroatoms such as tin impact zeolite crystallization. It has been previously shown that while pure silica zeolite beta takes only a couple of days, synthesizing Sn substituted beta typically requires over 20 days [40,41]. The method involving lower temperatures could be promising for producing Lewis acidic nano zeolites, but the effect of the tin species on the crystallization process is currently unknown. It is important to determine how the heteroatom inclusion changes the zeolite crystallization process, particularly since inclusion of Sn in crystallization of zeolite beta can inhibit crystallization. Since inhibiting nucleation can lead to fewer nuclei and leave more species available for growth, it may be difficult to generate Sn substituted zeolite nanocrystals.

The Sn-substituted nanozeolites may expand the scope of current chemical reactions, including our recent work involving epoxide ring opening with alcohols, as shown in Scheme 1 [42]. Epoxides are versatile and highly reactive chemical intermediates that can be ring opened to give variety of useful chemicals through nucleophilic attack by a range of nucleophiles, including nitrogen (e.g., amines [43–46]) and oxygen (e.g., water [47,48], alcohols [45], phenols [49], and  $CO_2$  [50]) containing species, leading to bifunctional molecules of great industrial value [51]. Of particular interest is epoxide ring opening with alcohols. The products obtained from ring opening of epoxides with alcohols are referred to as  $\beta$ -alkoxy alcohols. These are used as intermediates for the synthesis of several pharmaceutical compounds such as anti-tumor agents or immunosuppressives [52]. Our recent work indicates that reactions comprising bulky nucleophiles or epoxides are mass transfer limited [42], resulting in fast initial reaction rates that decrease with time and cause incomplete conversion of the epoxide. Overcoming these diffusion limitations would greatly expand the viable substrate scope for zeolites.

The present work investigates the effect of tin inclusion on the crystallization of nano sized MFI zeolites using a commercially available SDA. The particle size is monitored with DLS to determine the growth behavior at low temperature of pure silica and tin substituted MFI nanoparticles. The crystallized materials are characterized using standard techniques to understand the morphology, particle size, crystallinity, and composition of the resultant materials. The nano-zeolite catalysts are compared to MFI materials made using conventional synthesis conditions for epoxide ring opening reaction of 1,2-epoxyhexane and epichlorohydrin with methanol. The reusability and stability of Sn substituted nano-MFI zeolites is tested by performing recycle experiments.

### 2. Experimental Methods

#### 2.1. Chemicals

All the chemicals are used as received without any further purification. The following chemicals are used: tetraethyl orthosilicate (TEOS, reagent grade, 98%, Acros Organics), tetrapropylammonium hydroxide (TPAOH, 40 wt% solution in water, EMD Millipore), epichlorohydrin (99%, BeanTown Chemical), 1,2-epoxyhexane (97%, Acros Organics), methanol (HPLC grade, Fisher Chemical), diethylene glycol dibutyl ether (DGDE, >98%, TCI), and tin (IV) chloride pentahydrate (SnCl<sub>4</sub>•5H<sub>2</sub>O, 98%, Alfa Aesar). Deionized (DI) water is obtained from a house supply.

### 2.2. Catalyst Synthesis

# 2.2.1. Nano-MFI Synthesis

Pure silica MFI is synthesized through using a procedure similar to previous literature [34]. In the synthesis of Sn-substituted nano MFI material, TEOS is mixed with TPAOH solution to form the precursor synthesis gel. The mixture is prepared by using 20.81 g of TEOS, 18.30 g

of TPAOH, and 29.77 g of DI water. In a separate vial, 0.13 g of SnCl<sub>4</sub>•5H<sub>2</sub>O is mixed with 1.0 g of DI water and is added to the TEOS/TPAOH mixture to give a molar ratio of the precursors of 1 TEOS: 0.005 Sn: 0.36 TPAOH: 23 H<sub>2</sub>O. The synthesis gel is hydrolyzed for 24 hours with stirring at room temperature and is then heated by submerging the flask in an oil bath, pre-heated to the desired temperature. The materials are allowed to crystallize for six days. The crystals are diluted with DI water and separated using centrifugation at 8500 rpm (Beckman Coulter Alegra X - 30 centrifuge equipped with F0850 rotor model). After drying overnight, the materials are calcined at 560°C for 3 hours in air. For monitoring crystal growth with crystallization time, samples are extracted from the mixture at fixed time points and cooled to room temperature before analysis using DLS. Synthesis are performed at 60°C, 80°C, and 100°C. Correspondingly, the naming convention used for these samples is Sn200-nano-MFI-60C, Sn200-nano-MFI-80C, and Sn200-nano-MFI-100C, respectively.

# 2.2.2. Conventional MFI Synthesis

The conventional Sn-MFI material is synthesized using two methods. In the first method, the procedure reported in literature is used [53]. Briefly, a solution is prepared using 0.044 g of SnCl<sub>4</sub>•5H<sub>2</sub>O, 1.67 g of DI water, and 5.204 g of TEOS in a Teflon reactor. After stirring for 30 minutes, 11 g of TPAOH (20% wt. aq., the 40 wt% solution is diluted to achieve desired concentration) is added dropwise to the solution before mixing for an additional 1 hour. To the solution is added 4.67 g DI water before stirring for 30 minutes. The final molar composition is 1.0 TEOS: 0.005 Sn: 0.43 TPAOH: 33.6 H<sub>2</sub>O. In the second method, the synthesis gel is prepared with a composition of 1.0 TEOS: 0.005 Sn: 0.36 TPAOH: 23 H<sub>2</sub>O that is the same as the material synthesis mentioned in nano-MFI synthesis section. The mixture is hydrolyzed for 24 hours at room temperature. For both conventional methods, the subsequent procedure is the same. The

oven preheated to 160°C for 17 days under static conditions. The crystals obtained are washed with DI water several times and are separated using the centrifuge at 8500 rpm. After drying overnight at 80°C, the material is calcined at 560°C for 12 hours in air. The naming convention used for these materials is Sn-conventional-MFI-d and Sn-conventional-MFI-c for the material with dilute (Si:H<sub>2</sub>O of 1:33.6) and concentrated (Si:H<sub>2</sub>O of 1:23) crystallization conditions, respectively.

### 2.3. Material Characterization

1

2

3

4

5

6

7

8

9

10

11

12

13

14

15

16

17

18

19

20

21

22

23

24

The catalytic materials are analyzed using several characterization techniques, including nitrogen physisorption, powder X-ray diffraction (PXRD), scanning electron microscopy (SEM), dynamic light scattering (DLS), diffuse reflectance infrared fourier transform spectroscopy (DRIFTS), diffuse reflectance ultra-violet visible spectroscopy (DRUVS), thermogravimetric analysis-differential scanning calorimetry (TGA-DSC), and elemental analysis. The textural properties are characterized using a Micromeritics 3Flex surface characterization analyzer. The samples are first degassed on Micromeritics SmartVacPrep sample preparation device at 200°C under vacuum (10<sup>-5</sup> mmHg) for 15 h followed by in-situ degassing of samples on the 3Flex instrument for 3 h at 140°C under vacuum (5x10<sup>-5</sup> mmHg). The nitrogen sorption isotherms of degassed samples are recorded at liquid nitrogen temperatures (~77 K). The surface area and micropore volume of the materials are reported using BET and t-plot method, respectively. PXRD is performed on Bruker powder X-ray diffractometer using 40 kV, 40 mA, and room temperature in flat plate reflection, Bragg Brentano optics mode. The particle size and the morphology of the materials is analyzed using a FEI Nova 400 NanoSEM. SEM samples are prepared through dispersing the calcined material in ethanol before the mixture is dispersed on conductive carbon tape at 3000 rpm. The samples are sputter coated with ~8 nm thick layer of gold-palladium alloy using EMS 150T S sputter coater. DLS is performed using the Brookhaven Instruments

Corporation's BI-200SM dynamic light scattering instrument ( $\lambda$ =634 nm; scattering angle of 90°). Samples are extracted periodically from the different crystallization solutions and are analyzed as an aqueous suspension. Samples extracted during initial crystallization time did not require dilution; however, the samples extracted during the later stage are turbid, requiring dilution with MilliQ water before analysis. For specific data points for which large dust particles are observed, the samples are filtered using 0.2 µm nylon syringe filters before analyzing with DLS. DRIFTS is performed using a Nicolet iS50 spectrometer equipped with MCT-A liquid nitrogen cooled detector (32 scans at 2 cm<sup>-1</sup> resolution). The DRIFTS set up includes a Praying Mantis (Harrick Scientific products Inc.) with a high temperature reaction chamber consisting of zinc selenide (ZnSe) windows. The material is initially degassed in situ at 500°C for 90 minutes under nitrogen flow. The material is then cooled to 25°C and pulsed with deuterated-acetonitrile. [54] The probe molecule is allowed to desorb under nitrogen flow. The IR spectra are collected at room temperature under nitrogen using the material before dosing as the background. The DR-UV-vis spectra are collected on Evolution 300 UV-Vis spectrometer with a resolution of 2 nm at a rate of 10 nm/s with pure silica analogues of materials as the background. TGA is performed on a STA 449 F5 Jupiter® (NETZSCH instruments) under flowing air (20 mL/min) and nitrogen (20 mL/min) at a ramp rate of 10°C/min from 30°C to 900°C followed by a 5 min hold at 900°C. All the materials are characterized for elemental analysis by Galbraith Laboratories using inductively coupled plasma-optical emission spectroscopy (ICP-OES) to determine the weight percent of Sn substituted in the silica framework.

### 2.4. Catalytic Testing

1

2

3

4

5

6

7

8

9

10

11

12

13

14

15

16

17

18

19

20

21

22

23

24

The catalytic testing is carried out in a two neck 10 mL round bottom (RB) flask equipped with a condenser, a magnetic stir bar, and a septum. The RB is filled with 2 mL of a solution containing 0.4 M epoxide and diethylene glycol dibutyl ether (DGDE) as an internal standard in

neat alcohol. A sample (40 μL) is taken and diluted with acetone (~2 mL) to serve as the initial concentration data point. The required amount of catalyst to achieve an epoxide:Sn of 250:1 is then added to the RB. After adding the catalyst, the RB is immersed in a silicone oil bath, preheated to a temperature of 60°C. At specific times, a sample (40 μL) is withdrawn from this mixture using a reusable stainless-steel needle and is filtered using a small plug of silica, diluting with acetone. The samples are analyzed using gas chromatography (Agilent, 7820A) equipped with flame ionization detector (GC-FID) and the products are identified using GC-MS (equipped with Agilent HP-5ms Ultra Inert column) using positive ion mode electron ionization. The GC-MS data is reported in table S-1 for all the products observed. The conversion is computed using the internal standard method.

#### 3. Results and Discussion

# 3.1. Synthesis and Material Characterization

Initial work focuses on understanding differences between crystallization timescales for pure silica and tin substituted nano MFI crystals. Based on literature methods, pure silica nano crystals are first synthesized at 80°C [34,35]. The pure silica material obtained is separated through centrifugation and characterized using nitrogen physisorption (Figure S1) and PXRD (Figure S2). It is determined that the materials are fully crystalline after six days. For all materials presented, the fully crystallized materials are similar in quality. Details of the characterization are presented in Table 1.

The growth of the particles during synthesis is monitored by extracting samples at different times during crystallization and analyzing the samples using DLS to determine particle size as a function of time, as shown in Figure 1. As a base case, the particle growth at 80°C is monitored. After 24 hours, DLS measurements indicate a particle size of 30 nm. The particle size continues to increase with time in an approximately linear manner until a particle size of 76 nm

is obtained after three days. After this, the particle size remains constant indicating that an equilibrium has been reached between the particles and the growth solution [55]. Analysis of these samples with SEM determined a particle size of 65 nm (Figure 2), which is similar to DLS measurements. The discrepancy in size is possibly associated with the fact that DLS analysis is performed on materials in solution whereas SEM analysis is performed on calcined samples after depositing on a conductive carbon tape. Overall, this observed behavior is similar to previous work investigating the low temperature synthesis [34], and demonstrates that particle size can be monitored using DLS.

In synthesis of nanomaterials, it is important to balance final particle size and rate of crystallization; these have been shown to be affected by the crystallization temperature [34]. The effect of temperature on crystallization is confirmed through investigating two other synthesis temperatures 60°C and 100°C. First, the growth rate is strongly affected by the reaction temperature. As indicated from Figure 1, the growth rate increases with increasing temperature. At a temperature of 60°C, the material slowly grows, requiring approximately 350 hours (~15 days) to achieve a steady state particle size of 57 nm. The steady state particle size varies little over time, suggesting that material losses its driving force for growth at this concentration. For higher temperatures, the materials nucleate and grow in much shorter periods of time. At 100°C, the steady state particle size is reached in as little as 30 hours. Since higher temperature increases growth rate, it also affects the final measured particle size. Indeed, it is observed that the final particle size obtained increased with increasing temperature, as shown in Table 2. These results for pure silica are in agreement with previous studies examining the growth of MFI nanocrystals [34,35].

While the growth behavior for pure silica zeolites has been studied, the effect of introducing heteroatoms such as Sn has not been studied previously. For all data reported in

it is observed that the crystallization in the presence of Sn proceeded at a similar rate as the pure silica materials at all temperatures. The material growth follows a similar trend and addition of Sn had minimal impact on growth rate. One notable observation is that the growth at 60°C in the

Figure 1, the amount of Sn included in the synthesis is held fixed at a Si:Sn of 200:1. Interestingly,

5 presence of Sn results in larger particles than when Sn is absent. This suggests that fewer particles

nucleate in the presence of Sn at this temperature, leaving more silicon and tin species available

for growth to larger sizes.

The particle size is also analyzed using SEM for Sn-substituted nano material, as shown in Figure 2. The comparison of the sizes calculated using DLS and SEM is given in Table 2. The particle size calculated from DLS is in agreement with the particle size determined using SEM images. For the concentrated synthesis gel conditions (Sn200-conventional-MFI-c), the particle size is determined using SEM to be 220 nm (Figure 3) whereas the more dilute synthesis (Sn200-conventional-MFI-d) produced particles of 480 nm. The smaller particles observed for Sn200-conventional-MFI-c are because of the greater supersaturations, which would result in an increased nucleation rate as compared to Sn200-conventional-MFI-d.

The Sn containing nano and conventional materials are characterized using PXRD and nitrogen physisorption to confirm the formation of high quality MFI crystals. PXRD patterns for nano and conventional MFI samples are identical, and the peaks match with characteristic reference peaks of crystalline MFI structure indicated in Figure S2. Nitrogen physisorption isotherms are used to determine the surface area and micropore volume of nano and conventional MFI material (Table 1). The conventional material exhibits a type I isotherm and the values for micropore volume and surface area are in good agreement with the reported values [53]. Relative to the conventional materials, the nanomaterials are found to have greater external surface area, as would be expected. Additionally, these materials adsorb more nitrogen in the micropore region

 $(P/P_o<0.2)$  than the conventional materials and exhibit hysteresis at  $P/P_o\sim0.9$  that indicates the presence of large pores. This is consistent with the idea that nanoparticle aggregation creates interparticle voids in the material [56].

Elemental analysis is used to determine the amount of tin incorporated in the material, as shown in Table 1. For the conventional materials, the tin incorporation efficiency is expected to be relatively high [57], achieving a Si:Sn of 210:1 for Sn200-conventional-MFI-c and 252:1 for Sn200-conventional-MFI-d that is similar to the theoretical value of 200:1. Interestingly, the Sn incorporation in the nano material is lower than the conventional material giving higher Si:Sn than the targeted value of 200:1 across all samples synthesized at lower temperatures. For purposes of comparing catalyst performance, catalysts are synthesized using the conventional procedure with a Si:Sn of ~700:1 for both the dilute (Sn700-conventional-MFI-d) and concentrated (Sn700-conventional-MFI-d) procedures.

The materials are further characterized using DRIFTS and DRUVS to determine whether the Sn is incorporated as framework Sn or extra-framework tin oxide (SnO<sub>2</sub>) species. While <sup>119</sup>Sn NMR can indicate Sn coordination [58–60], the low concentrations for Sn would require multiple days to analyze. The presence of framework Sn sites has previously been confirmed through DRIFTS analysis with deuterated acetonitrile as the probe molecule, as has been previously reported [54]. As shown in Figure S3, all materials have a DRIFTS spectrum that has a peak at 2274 cm<sup>-1</sup> that is associated with the probe molecule adsorbing on silanols and a peak at 2309 cm<sup>-1</sup> that indicates the probe adsorbed on Lewis acidic Sn species in the material. This suggests that all materials have framework Sn sites. The materials are also analyzed with DRUVS since this method has previously been used to identify the formation of SnO<sub>2</sub> in the material [61]. The Sn species can exist in either tetrahedral coordination in the zeolite framework or as extra-framework Sn species typically seen as SnO<sub>2</sub> species residing on the catalyst surface. The extra-framework

SnO<sub>2</sub> species can give rise to a peak at 280 nm, as shown in Figure S4c. For the materials produced using the conventional synthesis methods, the tail of a peak could be observed at 200 nm that is commonly associated with framework tin species and does not contain a peak associated with SnO<sub>2</sub> (Figure S4a). The nano zeolites have similar DRUVS, but also include a small peak in the region for SnO<sub>2</sub> (Figure S4b). While this suggests a small amount of SnO<sub>2</sub>, the DRUVS spectra does have a shoulder around 200 nm that is more intense than the peak at 280 nm, which suggests that most of the Sn is coordinated in tetrahedral state. Coupled with DRIFTS analysis, this work indicates that most of the Sn present in the material are framework species.

# 3.2. Catalytic Testing

The nano and conventional materials are tested for catalytic activity using epoxide ring opening with an alcohol as a model reaction. Initial work examines the epoxide ring opening of epichlorohydrin with methanol. The expectation is that these substrates are sufficiently small molecules that they can react without diffusion limitations. As shown in Figure 4, catalytic testing experiments with Sn700-conventional-MFI-d results in complete conversion in less than 24 hours with an initial turnover frequency (TOF<sub>0</sub>) of 98 moles epoxides per mole Sn per hour. Catalytic activity is similar for Sn700-conventional-MFI-c, which is determined to have a TOF<sub>0</sub> of 104 moles epoxide per mole Sn per hour. These results are similar to our previous work for Sn-MFI [42]. The catalytic results for Sn200-nano-MFI-80C are similar to the conventional Sn-MFI; Sn200-nano-MFI-80C results in complete conversion in less than 24 hours with a TOF<sub>0</sub> of 91 moles epoxides per mole Sn per minute. The TOF<sub>0</sub> for the nano zeolite is slightly lower than the Sn700-conventional-MFI-d. The discrepancy is likely associated with small amounts of SnO<sub>2</sub> that has been demonstrated to have significantly lower catalytic activity than framework Sn sites [42], but the TOF<sub>0</sub> are sufficiently similar to investigate the effect of diffusion limitations for other epoxide ring opening reactions. In addition to activity, these catalysts exhibit similar

regioselectivity, producing 97% of the terminal ether (product 3 in Scheme 1). The similarity demonstrates that the low temperature synthesis produces materials with similar quantities of catalytic sites that have similar catalytic behavior. These catalysts can therefore be used to determine if diffusion limitations are impacting overall conversion for large substrates or whether the catalyst is deactivating [62].

1

2

3

4

5

6

7

8

9

10

11

12

13

14

15

16

17

18

19

20

21

22

23

The effect of particle size on diffusion limitations is analyzed using a reaction mixture consisting of an epoxide substrate 1,2-epoxyhexane and methanol. For all the tests, the reaction system consisted of the same epoxide:Sn of 250:1 with the amount of Sn based on elemental analysis. The reaction is first investigated through examining Sn200-conventional-MFI-d, as shown in Figure 5. This material achieves a 1,2-epoxyhexane conversion of 58% with regioselectivity of 61% for the terminal ether in 24 hours. While the initial reaction rate is fast, the rate slowed considerably after the first hour. This observed behavior is similar for Sn700conventional-MFI-d, which has fewer Sn sites and a larger particle size than Sn200-conventional-MFI-d, and Sn700-conventional-MFI-c, which has a particle size of 220 nm (Table 2) according to SEM analysis (Figure 3c). Both catalysts display similar regioselectivity for the terminal ether (59% for Sn700-conventional-MFI-d and 63% for Sn700-conventional-MFI-c) with the conversion of 1,2-epoxyhexane reaching ~65% conversion in 24 hours. The similarity in behavior suggests that diffusion limitations persist for this reaction even to particle sizes of 220 nm. The significant drop in rate might be caused by filling of pores that blocks accessibility to the active sites, decreasing the effectiveness of the catalytic material. After the reaction, the material is separated through centrifugation and dried in a low temperature (80°C) sample oven prior to analysis with TGA-DSC (Figure S5). TGA-DSC revealed a significant mass loss in the temperature range of 200 - 500°C, consistent with the presence of organic species in the pores.

Interestingly, catalytic testing with Sn200-nano-MFI-80C shows that the nano material exhibits significantly higher overall conversion at all times during the reaction, achieving a conversion of 1,2-epoxyhexane of >95% within 24 hours. At final conversion, the regioselectivity is observed to be 56% for the terminal ether, which is comparable to Sn200-conventional-MFI-d. The increase in catalytic activity is attributed to faster diffusion of reactants and products into and out of the nano material. While the results cannot rule out diffusion limitations for nano zeolites, the data suggest that internal mass transfer processes are limiting the observed conversion for the conventional MFI catalysts.

The successful complete conversion of larger substrates in the Sn-nano-MFI materials is promising provided that the materials can be reused in several catalytic cycles. Recycle experiments are performed through testing the nano-MFI catalyst with the epoxide ring opening reaction of 1,2-epoxyhexane with methanol. These experiments involve recovering the catalyst after each cycle and are more easily accomplished through scaling up all components of the reaction by a factor of three to increase the amount of catalyst that can be recovered while maintaining the ratio of epoxide:Sn of 250:1. For this larger scale, the catalytic results for the nano-MFI during the first cycle is similar to reactions performed at smaller scales, as shown in Figure 6. After the first cycle, the catalyst is separated through centrifugation and is washed with 20 mL of methanol. The catalyst is dried before testing in a second cycle. For the second cycle, the recovered catalyst is weighed, and the amount of reaction mixture is scaled to maintain an epoxide:Sn of 250:1. The recovered catalyst appears to have lower activity than the fresh catalytic material, as shown in Figure 6. This apparent catalytic activity further decreases for the third cycle of the catalytic material.

This decrease in catalytic activity could be associated with either loss of catalytic sites or accumulation of organic content. Examining the catalyst with thermogravimetric analysis after

the third cycle reveals a mass loss of approximately 8%, as shown in Figure 7. The accumulation of organic content would impede further reaction from occurring. Therefore, it is investigated if the catalytic activity can be recovered through calcination of the accumulated organic species. After calcination, the amount of tin remaining in the material is determined using elemental analysis and is found to be 0.263 wt%. It is determined that the Si:Sn remains similar after three catalytic cycles and calcination, indicating that loss of catalytic sites through leaching is not a significant cause for catalyst deactivation. Indeed, testing the calcined catalyst in a fourth catalytic cycle reveals that the calcined catalyst has similar initial catalytic activity and regioselectivity as the fresh catalytic material. This indicates that organic accumulation in the pores impacts the catalyst reusability, but the decrease in activity can be reversed through calcination. This result is consistent with recycle experiments for Sn-substituted zeolites used in the epoxide ring opening with alcohols that demonstrated Sn did not leach from the framework [42]. At longer reaction times, the difference in conversion is likely associated with small differences in catalytic activity that are amplified by product diffusion out of the material. Overall, these results indicate that the nanometer size of the MFI zeolites are robust catalytic materials.

# 3.3. Strategies to Increase Framework Tin Content

The catalytic activity for 1,2-epoxyhexane conversion for the Lewis acidic nano-MFI zeolite is greater than its conventional counterpart. However, one of the limitations encountered in synthesizing such nano material is significantly lower heteroatom incorporation within the material than the theoretical targeted amount. This is evidenced in the elemental analysis results, where the actual Si:Sn ratio obtained for the material is 724:1, while the theoretical ratio is 200:1. To overcome this challenge two strategies are investigated. First, the synthesis is carried out at higher temperature of 100°C to understand how the synthesis temperature affects Sn incorporation in the material. Secondly, more tin is added to decrease the theoretical Si:Sn to

50:1, keeping the synthesis temperature at 80°C. It is observed that increasing the synthesis temperature to 100°C has a minor effect on the amount of Sn incorporated (theoretical Si:Sn = 200:1; actual Si:Sn = 775:1) in the material (Sn200-nano-MFI100C). This suggests that there is a threshold temperature at which Sn is more readily incorporated into the zeolite framework since the conventional material synthesized at 160°C has higher Sn incorporation, as indicated in Table 1. The alternative strategy of adding more Sn to the synthesis gel results in increased Sn incorporation into the final material, achieving a Si:Sn of 110. This material is analyzed using SEM, determining that the particle size is 85 nm. This particle size is similar to the pure silica and Si:Sn of 200:1 materials, indicating that the synthesis temperature has the largest impact on particle size. This material (Sn50-nano-MFI-80C) is tested for the epoxide ring opening of 1,2epoxyhexane with methanol and in 24 hours 91% conversion is observed with 53% regioselectivity for terminal ether. The observed conversion over time behavior as well as the regioselectivity at final conversion do not differ significantly than Sn200-nano-MFI-80C, indicating that larger amounts of tin can be incorporated into the nano zeolite to produce a highly active catalytic material. Overall, these results demonstrate that controlling the particle size can improve the overall catalytic performance of Lewis acidic zeolites.

# 4. Summary

1

2

3

4

5

6

7

8

9

10

11

12

13

14

15

16

17

18

19

20

21

22

23

24

Synthetic conditions have been identified to produce Sn containing nano MFI zeolites using a commercial SDA. It is observed that the low temperature synthesis conditions produced a five-fold reduction in particle size compared to MFI crystals produced using conventional hydrothermal methods. At a Si:Sn of 200:1, the particle growth monitored by DLS shows minimal effect of Sn addition on crystallization growth rate, but resulted in low amounts of tin incorporation into the material. The characterization of the materials revealed crystalline structures with framework Sn species. For small substrates, the nano and conventional materials

- 1 have similar catalytic activity. Sn-nano-MFI when tested for ring opening of 1,2-epoxyhexane
- 2 with methanol shows enhanced catalytic activity compared to the conventionally synthesized
- 3 material. The nano zeolites can be reused directly, but organic accumulation in the pores
- 4 necessitates calcination to maintain high catalytic activity.

# Acknowledgements

- We gratefully acknowledge the American Chemical Society Petroleum Research Fund
- 7 (ACS-PRF 55946-DNI5), the National Science Foundation (NSF Career 1653587), and the Ohio
- 8 State University Institute for Materials Research (OSU IMR FG0137 and EMR-G00018) for their
- 9 financial support.

# **Competing Interest**

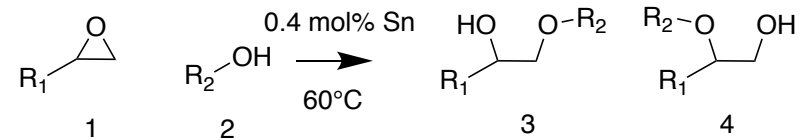
- The authors declare no competing interest.
- 12 13 14

10

#### References

- 2 [1] R.G. Konsler, J. Karl, E.N. Jacobsen, J. Am. Chem. Soc. 120 (1998) 10780.
- 3 [2] K. Venkatasubbaiah, C.S. Gill, T. Takatani, C.D. Sherrill, C.W. Jones, Chem. Eur. J. 15 (2009) 3951.
- 5 [3] N.A. Brunelli, S.A. Didas, K. Venkatasubbaiah, C.W. Jones, J. Am. Chem. Soc. 134 (2012) 13950.
- 7 [4] M.A. Camblor, A. Corma, S. Valencia, J. Mater. Chem. 8 (1998) 2137.
- 8 [5] T. Blasco, M.A. Camblor, A. Corma, P. Esteve, J.M. Guil, A. Martínez, J.A. Perdigón-Melón, S. Valencia, J. Phys. Chem. B 102 (1998) 75.
- 10 [6] R. Gounder, M.E. Davis, AIChE J. 59 (2013) 3349.
- 11 [7] R. Rodríguez, M.E. Davis, ACS Catal. 1 (2011) 1566.
- 12 [8] E.Y.-X. Chen, T.J. Marks, Chem. Rev. 100 (2000) 1391.
- 13 [9] M. Moliner, M. Moliner, Dalt. Trans. 43 (2014) 4197.
- 14 [10] A. Corma, L.T. Nemeth, M. Renz, S. Valencia Valencia, S. Valencia, Nature 1433 (2001) 423.
- 16 [11] A. Corma, M.E. Domine, L. Nemeth, S. Valencia Valencia, J. Am. Chem. Soc. 124 (2002) 3194.
- 18 [12] D.T. Bregante, D.W. Flaherty, J. Am. Chem. Soc. 139 (2017) 6888.
- 19 [13] J.D. Lewis, S. Van De Vyver, R. Rodríguez, S. Van de Vyver, Y. Román-Leshkov, Angew. Chemie Int. Ed. 54 (2015) 9835.
- 21 [14] M. Moliner, Y. Román-Leshkov, M.E. Davis, Proc. Natl. Acad. Sci. 107 (2010) 6164.
- 22 [15] W.R. Gunther, Y. Wang, Y. Ji, V.K. Michaelis, S.T. Hunt, R.G. Griffin, R. Rodríguez, Nat. Commun. 3 (2012) 1109.
- 24 [16] M. Orazov, M.E. Davis, Proc. Nat. Acad. Sci. 2015 (2015) 1.
- 25 [17] G. Perot, M. Guisnet, J. Mol. Catal. 61 (1990) 173.
- [18] J. Pérez-Ramírez, C.H. Christensen, K. Egeblad, C.H. Christensen, J.C. Groen, Chem.
  Soc. Rev. 37 (2008) 2530.
- 28 [19] S.S. Kim, J. Shah, T.J. Pinnavaia, Chem. Mater. 15 (2003) 1664.
- 29 [20] C.J.H. Jacobsen, C. Madsen, J. Houzvicka, I. Schmidt, A. Carlsson, J. Am. Chem. Soc. 122 (2000) 7116.
- 31 [21] C.H. Christensen, K. Johannsen, I. Schmidt, C.H. Christensen, J. Am. Chem. Soc. 125 (2003) 13370.
- 33 [22] J.C. Groen, W. Zhu, S. Brouwer, S.J. Huynink, F. Kapteijn, J.A. Moulijn, J. Pérez-34 Ramírez, J. Am. Chem. Soc. 129 (2007) 355.
- 35 [23] I. Ogino, M.M. Nigra, S.J. Hwang, J.M. Ha, T. Rea, S.I. Zones, A. Katz, J. Am. Chem.
  36 Soc. 133 (2011) 3288.
- 37 [24] Y. Tao, H. Kanoh, L. Abrams, K. Kaneko, Chem. Rev. 106 (2006) 896.
- F.C. Meunier, D. Verboekend, J.P. Gilson, J.C. Groen, J. Pérez-Ramírez, Microporous Mesoporous Mater. 148 (2012) 115.
- 40 [26] S. Van Donk, A.H. Janssen, J.H. Bitter, Catal. Rev. 45 (2013) 297.
- 41 [27] S. Mintova, N.H. Olson, V. Valtchev, T. Bein, Science 283 (1999) 958.
- 42 [28] S. Mintova, J.-P. Gilson, V. Valtchev, Nanoscale 5 (2013) 6693.
- 43 [29] M. Choi, K. Na, J.Y. Kim, Y. Sakamoto, O. Terasaki, R. Ryoo, Nature 461 (2009) 246.
- 44 [30] H.Y. Luo, L. Bui, W.R. Gunther, E. Min, Y. Roman-Leshkov, ACS Catal. 2 (2012) 2695.
- 46 [31] A.A. Rownaghi, J. Hedlund, Ind. Eng. Chem. Res. 50 (2011) 11872.
- 47 [32] T.F. Mastropietro, E. Drioli, T. Poerio, RSC Adv. 4 (2014) 21951.

- 1 [33] H. Konno, T. Okamura, T. Kawahara, Y. Nakasaka, T. Tago, T. Masuda, Chem. Eng. J. 207–208 (2012) 490.
- 3 [34] Q. Li, D. Creaser, J. Sterte, Microporous Mesoporous Mater. 31 (1999) 141.
- 4 [35] Q. Li, B. Mihailova, D. Creaser, J. Sterte, Microporous Mesoporous Mater. 40 (2000) 53.
- 6 [36] T.M. Davis, T.O. Drews, H. Ramanan, C. He, J. Dong, H. Schnablegger, M.A. Katsoulakis, E. Kokkoli, A. V Mccormick, R.L.E.E. Penn, M. Tsapatsis, Nat. Mater. 5 (2006) 400.
- 9 [37] G. Sankar, T. Okubo, W. Fan, F. Meneau, (n.d.).
- 10 [38] J.M. Fedeyko, J.D. Rimer, R.F. Lobo, D.G. Vlachos, J. Phys. Chem. B 108 (2004) 12271.
- 12 [39] R. Martínez-Franco, C. Paris, M.E. Martínez-Armero, C. Martínez, M. Moliner, A. Corma, Chem. Sci. 7 (2016) 102.
- 14 [40] S. Valencia Valencia, A. Corma, Stannosilicate Molecular Sieves, 1999.
- 15 [41] S. Tolborg, A. Katerinopoulou, D.D. Falcone, I. Sadaba, C.M. Osmundsen, R.J. Davis, E. Taarning, P. Fristrup, M.S. Holm, J. Mater. Chem. A 2 (2014) 20252.
- 17 [42] N. Deshpande, A. Parulkar, R. Joshi, B. Diep, N.A. Brunelli, (In Prep.) (n.d.).
- 18 [43] T. Baskaran, A. Joshi, G. Kamalakar, A. Sakthivel, Appl. Catal. A Gen. 524 (2016) 50.
- 19 [44] A.K. Shah, K.J. Prathap, M. Kumar, S.H.R. Abdi, R.I. Kureshy, N. ul H. Khan, H.C. Bajaj, Appl. Catal. A Gen. 469 (2014) 442.
- 21 [45] D. Bhuyan, L. Saikia, D.K. Dutta, Appl. Catal. A Gen. 487 (2014) 195.
- [46] A.K. Shah, M. Kumar, S.H.R. Abdi, R.I. Kureshy, N.U.H. Khan, H.C. Bajaj, Appl.
  Catal. A Gen. 486 (2014) 105.
- [47] W. Dai, C. Wang, B. Tang, G. Wu, N. Guan, Z. Xie, M. Hunger, L. Li, ACS Catal. 6
  (2016) 2955.
- 26 [48] B. Tang, W. Dai, G. Wu, N. Guan, L. Li, M. Hunger, ACS Catal. 4 (2014) 2801.
- 27 [49] N.A. Brunelli, W. Long, K. Venkatasubbaiah, C.W. Jones, Top. Catal. 55 (2012) 432.
- 28 [50] B.M. Bhanage, S.I. Fujita, Y. Ikushima, M. Arai, Appl. Catal. A Gen. 219 (2001) 259.
- 29 [51] R. Kore, R. Srivastava, B. Satpati, ACS Catal. 3 (2013) 2891.
- 30 [52] G. Prestat, C. Baylon, M.P. Heck, C. Mioskowski, Tetrahedron Lett. 41 (2000) 3829.
- 31 [53] C.M. Lew, N. Rajabbeigi, M. Tsapatsis, Microporous Mesoporous Mater. 153 (2012) 55.
- 32 [54] S. Roy, K. Bakhmutsky, E. Mahmoud, R.F. Lobo, R.J. Gorte, ACS Catal. 3 (2013) 573.
- 33 [55] A. Ghorbanpour, A. Gumidyala, L.C. Grabow, S.P. Crossley, J.D. Rimer, ACS Nano 9 (2015) 4006.
- 35 [56] C. Zhang, J.A. Gee, D.S. Sholl, R.P. Lively, J. Phys. Chem. C 118 (2014) 20727.
- 36 [57] M. Shahami, R. Ransom, D.F. Shantz, Microporous Mesoporous Mater. 251 (2017) 165.
- 37 [58] Y.G. Kolyagin, A. V. Yakimov, S. Tolborg, P.N.R. Vennestrøm, I.I. Ivanova, J. Phys. Chem. Lett. 7 (2016) 1249.
- 39 [59] W.R. Gunther, V.K. Michaelis, M.A. Caporini, R.G. Griffin, R. Rodríguez, J. Am. Chem. Soc. 136 (2014) 6219.
- 41 [60] S.-J. Hwang, R. Gounder, Y. Bhawe, M. Orazov, R. Bermejo-Deval, M.E. Davis, Top. Catal. (2015).
- 43 [61] R. Bermejo-Deval, R. Gounder, M.E. Davis, ACS Catal. 2 (2012) 2705.
- 44 [62] C.H. Bartholomew, Appl. Catal. A Gen. 212 (2001) 17.



**Scheme 1.** Epoxide ring opening reaction converting a terminal epoxide (1) with an alcohol (2) using a Lewis acidic catalyst (0.4 mol% Lewis acid - mostly Sn - and 60°C is used) to produce beta alkoxy alcohols with either a terminal ether (3) or a secondary ether (4).

**Table 1.** Material characterization of Sn substituted MFI zeolites, including textural properties and composition.

Sample	Surface	Micropore	Theoretical	Actual	%
	Area	volume	Sn (wt%)	Sn	Incorporation
	$(m^2/g)^a$	$(cm^3/g)^b$		(wt %) <sup>c</sup>	efficiency <sup>d</sup>
Sn200-nano-MFI-80C	521	0.15	0.978	0.272	28
Sn200-nano-MFI-100C	531	0.16	0.978	0.254	26
Sn50-nano-MFI-80C	594	0.14	3.802	1.64	43
Sn200-conventional-MFI-c	372	0.12	0.978	0.928	95
Sn200-conventional-MFI-d	388	0.13	0.978	0.776	79
Sn700-conventional-MFI-d	380	0.11	0.281	0.239	85
Sn700-conventional-MFI-c	387	0.13	0.281	0.263	94

<sup>&</sup>lt;sup>a</sup> Based on nitrogen physisorption, BET method. <sup>b</sup> Based on nitrogen physisorption, t-plot method.

<sup>&</sup>lt;sup>c</sup>Based on elemental analysis. <sup>d</sup>% incorporation efficiency calculated using the following formula

<sup>= (</sup>Actual Sn wt% / Theoretical Sn wt%)\*100

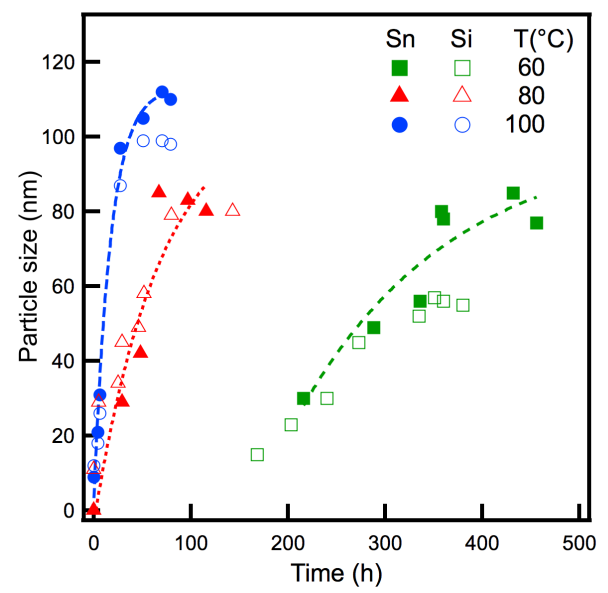


**Figure 1**. Comparison of the effect of synthesis temperature on particle size over time measured by DLS for both pure silica (open symbols) and tin containing (closed symbols) synthesis mixtures. The synthesis mixtures have an initial composition of 1 TEOS: 0.36 TPAOH: 23 H<sub>2</sub>O for pure silica or 1 TEOS: 0.005 Sn: 0.36 TPAOH: 23 H<sub>2</sub>O for tin containing mixtures. The mixtures are hydrolyzed at room temperature for 24 hours before the mixing is raised to the desired temperature.

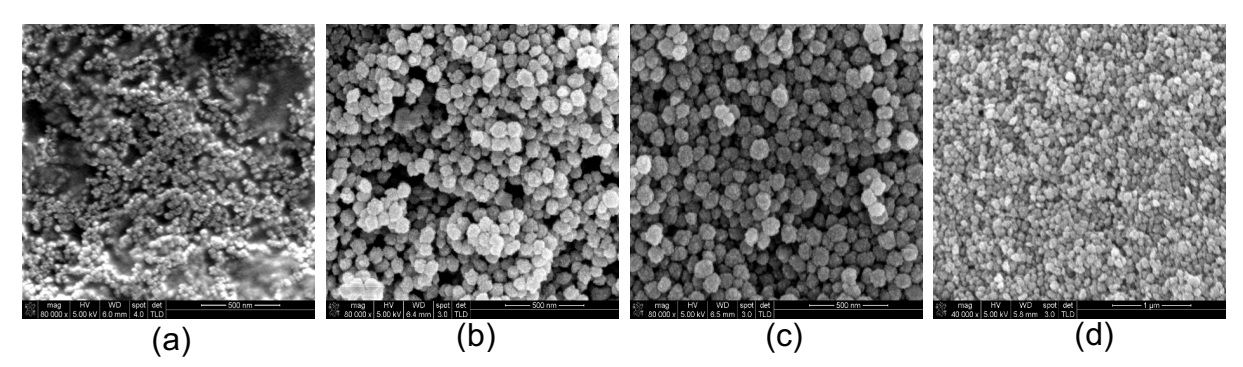


**Figure 2.** SEM images of samples of (a) Si-nano-MFI-80C as synthesized, (b) Sn200-nano-MFI-80C (calcined), (c) Sn200-nano-MFI-100C (calcined), and (d) Sn50-nano-MFI-80C (calcined).

**Table 2.** Comparison of particle sizes measured using Dynamic Light Scattering (DLS) and Scanning Electron Microscopy (SEM). DLS sample size corresponds to the apparent steady state size.

Sample	Particle size (nm)	Particle size (nm)
	DLS	SEM
Si-nano-MFI-80C	76	65
Sn200-nano-MFI-80C	90	95
Sn200-nano-MFI-100C	115	125
Sn50-nano-MFI-80C	90	85
Sn200-conventional-MFI-c	-	220
Sn200-conventional-MFI-d	-	480
Sn700-conventional-MFI-c	-	260
Sn700-conventional-MFI-d	-	20 μm

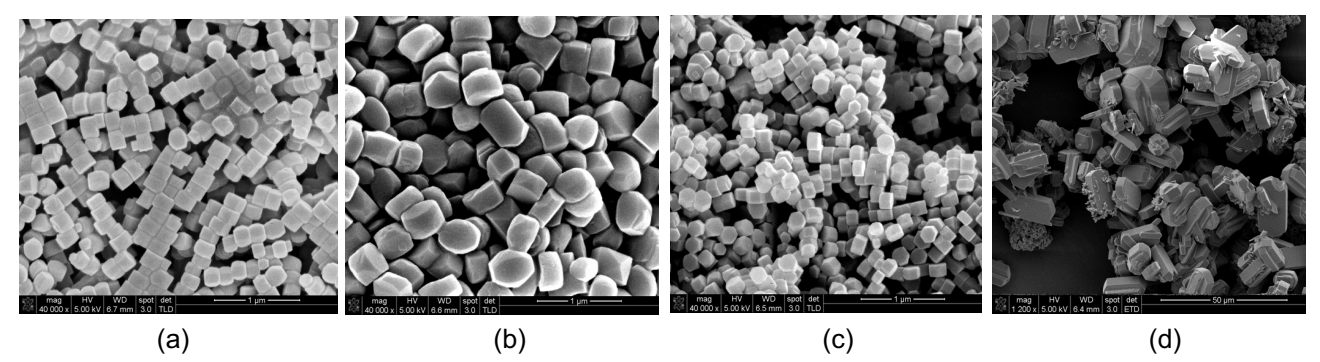


**Figure 3**. SEM images of conventional MFI samples: (a) Sn200-conventional-MFI-c, (b) Sn200-conventional-MFI-d, (c) Sn700-conventional-MFI-c, and (d) Sn700-conventional-d. Images a-c are shown at magnification of 1  $\mu$ m and image d is shown at magnification of 50  $\mu$ m.

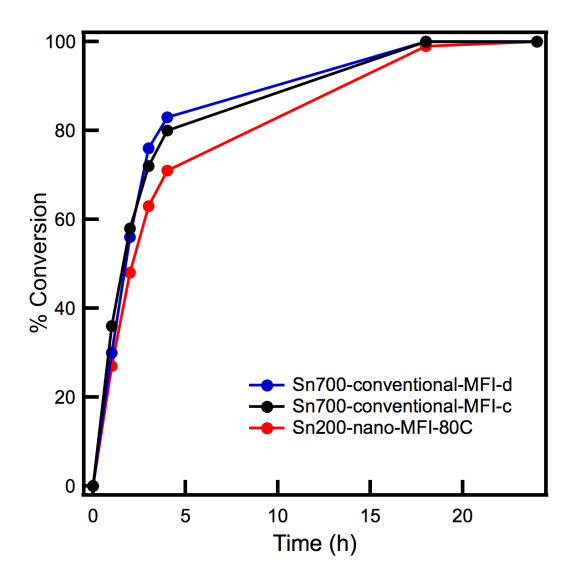


**Figure 4.** Comparison of conversion of epichlorohydrin with Sn-containing catalysts, Sn700-conventional-MFI-d (blue), Sn700-conventional-MFI-c (black), and Sn200-nano-MFI-80C (red). The amount of catalyst added is scaled to achieve an epoxide:Sn of 250:1. The reaction conditions are: 0.4 M epichlorohydrin in 2 mL methanol,  $10~\mu L$  DGDE (internal standard),  $60^{\circ}C$ , and 600 RPM.

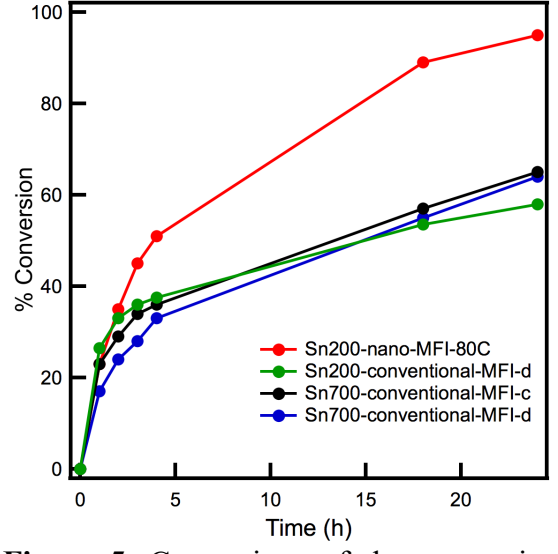


**Figure 5**. Comparison of the conversion of 1,2-epoxyhexane with Sn-containing catalysts, Sn200-nano-MFI-80C (red), Sn200-conventional-MFI-d (green), Sn700-conventional-MFI-c (black), and Sn700-conventional-MFI-d (blue). The amount of catalyst added is scaled to achieve an epoxide:Sn of 250:1. Reaction conditions: 0.4 M 1,2-epoxyhexane in 2 mL methanol, 30 μL DGDE (internal standard), 60°C, and 600 RPM.

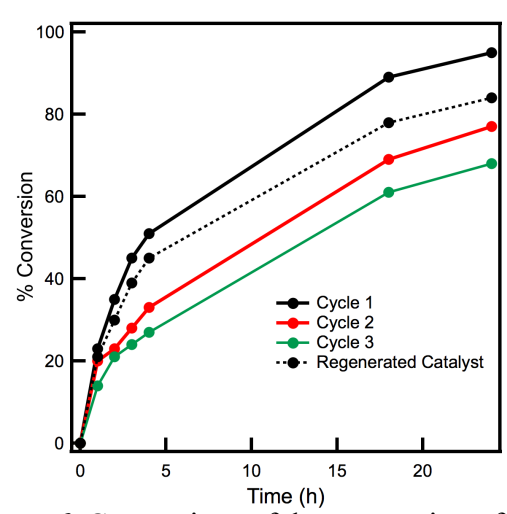


**Figure 6.** Comparison of the conversion of 1,2-epoxyhexane over time for Sn200-nano-MFI-80C for cycles of the catalyst reusability testing. Fresh catalyst is used for cycle 1 that is recovered via centrifugation and used in a second catalytic cycle. For each catalytic cycle, the amount of the reaction mixture (0.4 M 1,2-epoxyhexane in methanol with 0.06 M DGDE (internal standard)) is scaled to achieve an epoxide:Sn of 250:1. The reactions are performed at 60°C with a stirring speed of 600 RPM.

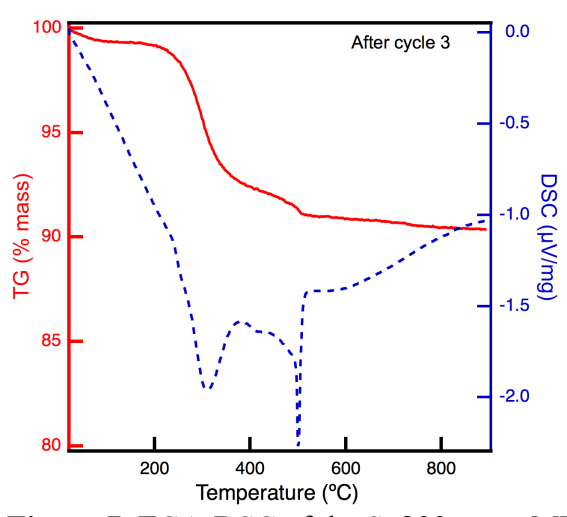


**Figure 7.** TGA-DSC of the Sn200-nano-MFI-80C catalyst recovered after three catalytic cycles. A mass loss of ~8% is observed because of accumulation of organic content in the pores. The solid line represents TG data and dotted line represents DSC data.

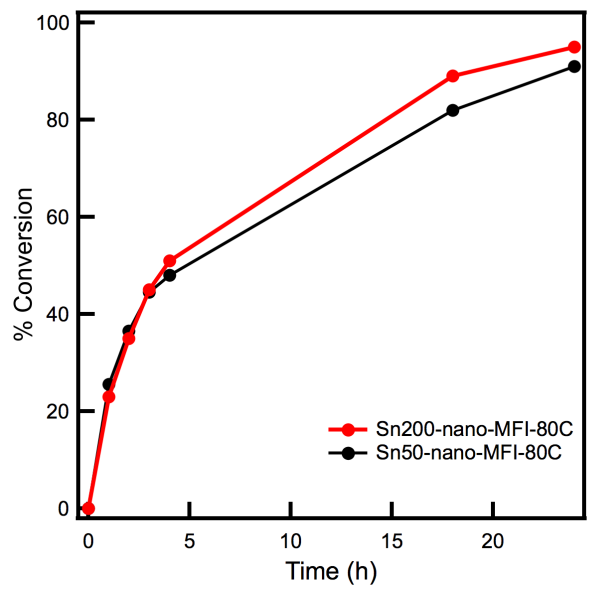


**Figure 8.** Comparison of the effect of Sn content on the catalytic activity using Sn200-nano-MFI-80C and Sn50-nano-MFI-80C. The amount of catalyst added is scaled to achieve an epoxide:Sn of 250:1. The reaction conditions are: 0.4 M 1,2-epoxyhexane in 2 mL methanol, 30  $\mu$ L DGDE (internal standard), 60°C, and 600 RPM.